Identification of the different diffuse dielectric barrier discharges obtained between 50 kHz to 9 MHz in Ar/NH 3 at atmospheric pressure

R Bazinette, R Subileau, J Paillol, Françoise Massines

Identification of the different diffuse dielectric barrier discharges obtained from 50 kHz to 9 MHz in Ar/NH_3 at atmospheric pressure

R. Bazinette[1],R. Subileau[2], J. Paillol[2], F. Massines[1]

[1] Laboratoire PROcédés Matériaux et Energie Solaire, UPR 8521, Tecnosud, 66100 PERPIGNAN, France
Telephone: +33(0)468682228; Fax: +33(0)468682213
Email: francoise.massines@promes.cnrs.fr
[2] SIAME, Université de Pau et des Pays de l'Adour

Abstract: The aim of this work was to identify the different diffuse dielectric barrier discharges (DBDs) obtained in the same electrode configuration and in the same gas for an excitation frequency ranging from 50 kHz to 9 MHz. The gas mixture was argon with 133 ppm of NH_3. This Penning mixture is useful to obtain both low frequency glow DBDs and diffuse radio frequency discharges. Electrical measurements and short exposure time photographs showed that whatever the frequency, a discharge free of micro-discharge was obtained. In the same configuration, the discharge was a glow DBD up to 200 kHz. For frequencies higher than 250 kHz, the discharge behavior was that of a Townsend-like discharge associated with a maximum energy transfer close to the anode and a higher power (about twice that of the glow DBD). The cathode fall formation was no longer observed during the discharge current increase because of ion trapping in the gas gap by the rapid electric field oscillations. In the same configuration, the alpha radio frequency mode was observed from 1.3 MHz. Gamma secondary electron emission gave way to electron acceleration by the cathode sheath formation. Bulk ionization was important due to the high electron collision rate at atmospheric pressure. One consequence of the transition from low frequency to high frequency discharge was a significant increase in the power (factor ≈30), which reached 35 W/cm^3, while the breakdown voltage decreased from 900 V to less than 200 V.

Keywords: Diffuse DBD, atmospheric pressure glow discharge, APGD, atmospheric pressure Townsend discharge, APTD, atmospheric pressure radio frequency discharge, alpha mode, noble gas DBD

1. Introduction

Atmospheric pressure diffuse or homogeneous discharges are streamer-free discharges. At atmospheric pressure, low frequency diffuse dielectric barrier discharges (DBDs) have been abundantly studied [1,2,3]. They are transient discharges, turning on and off during each half cycle. Two different regimes have been identified: atmospheric pressure glow discharge (APGD) or Glow DBD (GDBD), and atmospheric pressure Townsend discharge (APTD) or Townsend DBD (TDBD). APGDs are obtained in Penning mixtures of noble gases, and TDBDs in nitrogen or air. Both are free of micro-discharges, and are due to a Townsend breakdown related to memory effect and conditions allowing the breakdown voltage to be decreased and the ionization increase to be slowed. Memory effect is due to ions trapped by ambipolar field in APGDs, whereas in TDBDs, metastable species play the main role. Another difference is the maximum ionization level, which may or may not lead to ion accumulation close to the cathode, and then to the formation or non-formation of a cathode fall. The higher the ionization level is during each discharge pulse, the thinner is the cathode fall. In the glow mode the electron density reaches a value between 10^{10} and 10^{11} cm^{-3}, whereas in TDBD, it is 10^{7} to 10^{8} cm^{-3} [1]. However, the power is higher in a TDBD, mainly because of the larger ratio of the discharge time on to time off. Another discharge mode of high power has been pointed out [29]. This glow like regime is obtained with a special power supply.

Radio frequency homogeneous dielectric barrier discharges at atmospheric pressure (RFDBDs) have also been studied. Up to now they have mostly been observed in noble gases [4,5,6] He and Ar with and without dielectric on electrodes. In nitrogen however, gas heating is too high [7]. A Penning mixture is not necessary to obtain an RF diffuse discharge. Ionization mechanisms are the same as for low pressure and atmospheric pressure RF discharge [4, 5, 6]. Alpha and gamma modes are observed. In the alpha mode, ionization occurs partly in the bulk and partly at the edge of the plasma bulk by wave-riding, where interaction between cold electrons from bulk and the sheath motion produce electron heating. Bulk electrons are usually weakly heated because of the low value of the local electric field; nevertheless, this ohmic heating is sufficient to sustain the plasma. According to the literature, at atmospheric pressure, electron heating in the bulk is the main mechanism; however, depending on the experimental set-up (frequency, nature of the gas, etc.), two characteristic bright thin layers near electrodes can appear in addition, indicating electron heating at the interface between the sheath and the bulk. At atmospheric pressure, like at low pressure, if the power increases, alpha-gamma transition occurs. This is due to sheath gas breakdown allowing strong cathode bombardment and secondary electron emission. Discharge constriction induced by the transition to gamma mode is usually avoided by covering the electrodes with a solid dielectric, leading to RFDBD [5, 8]. At 150MHz, homogeneous plasma have also been observed without dielectrics [28].

Much work has been done with frequency excitations lower than 100 kHz and higher than 10 MHz, but the range in between has been under-researched. This work, for which the ultimate purpose is to increase the

power of homogeneous DBDs, helps to address this lack. There would be many more technological applications of diffuse DBDs if their power was higher [9]. Discharge filamentation limits the applied voltage or the discharge current. This lack of power slows down the processes, hampering technological development. As low frequency DBDs are pulsed discharges, we might expect that the higher the discharge repetition rate, i.e. the excitation frequency, the higher would be the power. However, discharge development and regime are also influenced by the excitation frequency. The aim of this work was to determine how the physics of diffuse discharge changes with excitation frequency, and how this affects their power. To this end, measurements were made for excitation frequencies ranging from 50 kHz to 9 MHz in the same atmosphere and in the same reactor.

Argon with a low concentration of ammonia, being a Penning mixture suitable for both GDBD [1] and RFDBD, was the gas mixture chosen for this study. The electrode configuration was plane/plane with the two electrodes covered with a dielectric layer, and the gas gap was 1 mm.

After a description of the experimental set-up, the different discharge regimes are identified through electrical measurements and high speed photography.

2. Experimental set-up

Figure 1 is a schematic view of the experimental reactor with two regions areas defined by the two high-voltage electrodes metalized on an internal face of dielectric square tubes (99% Al_2O_3) 3 mm thick.

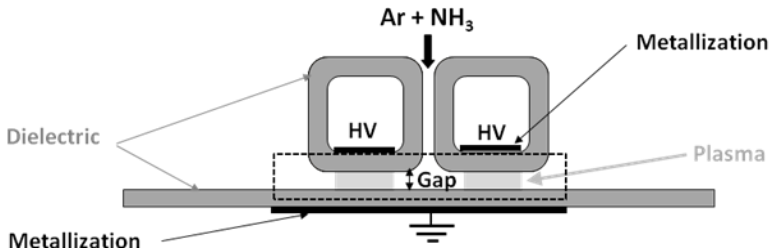

Figure 1. Discharge cell set-up

The ground electrode is on the other side of the one-millimeter gap. It is also covered with an alumina plate (96% Al_2O_3) 3 mm thick. The metallization area is twice 14×50 mm² for high voltage electrodes and 50×50 mm^2 for the low voltage one. In this work, the gap was set at 1 mm, which is suitable for GDBDs and RFDBDs at atmospheric pressure.

The discharge cell is an airtight reactor. The ambient air was removed with a primary vacuum, and the reactor was filled with argon up to a pressure of 760 torr (Alphagaz argon 2, less than 500 ppb of impurity). The gas was introduced through a 50 mm slit between the two square tubes 1.5 mm apart. This configuration ensures a laminar gas flow without recirculation in the plasma zones [10]. The Ar flow rate

was set at 3 l/min by a mass flow controller. NH_3 was mixed with Ar before it entered the reactor. Its concentration was set at 133 ppm.

The electrical device that applies a sinus form voltage to the DBD interelectrode gap consisted of a waveform generator connected to an amplifier. Since the voltage at the output of the amplifier was not sufficient to ignite a discharge, the amplifier output was fed into a high voltage transformer.

Up to 60 kHz, an audio amplifier was used (Crest Audio CC4000), and a high voltage transformer with a large bandwidth. The maximum available voltage was 3 kV. The large bandwidth of 1 kHz to 60 kHz was obtained with a ferrite magnetic core. The circuitry allowed voltage and frequency to be independently adjusted.

At higher frequencies, magnetic losses are too great to ensure a sufficient voltage gain. In this case an air core transformer is one possible technical solution. It is made of two windings of n_1 and n_2 turns at the primary and the secondary ports. The ratio n_2/n_1 was made greater than 1 to ensure voltage amplification. The resistance of the secondary windin, R_s, is in series with the capacitive load C_{DBD}, which stands for the capacitance of the DBD interelectrode gap. Note that this kind of homemade transformer has to be designed to match the 50 Ω output of the RF amplifier in order to obtain maximum P_{in}. However sufficient voltage gain amplification and a suitable tuning can, only, be obtained for a very narrow bandwidth. That is around the resonance frequency of the circuit made of the self-inductance of the secondary winding, its resistance and the capacitance of the DBD interelectrode gap in series. The frequency is adjusted to be close to the perfect match defined by Equation 1. The discharge cell can be modeled by an equivalent capacitor, $C_{DBD} \approx 10$ pF. These different elements form an oscillating circuit defined by Equation 1:

$$f_s = \frac{1}{2\pi\sqrt{L_s C_{DBD}}} \qquad \text{Equation 1}$$

The frequency of the generator waveform was varied around f_s to benefit from the resonance phenomenon, i.e. to maximize the power injected in the discharge and minimize the power reflected to the generator.
With five transformers, the available frequencies were therefore: 140 kHz, 200 kHz, 250 kHz, 550 kHz, and 800 kHz, 1.5 MHz, 1.7 MHz, 3 MHz, 4.4 MHz, 5.5 MHz, 8 MHz and 9.2 MHz. The amplifier was a PRANA amplifier model GN500 working between 100 kHz and 200 MHz with a maximum power of 500 W.

The plasma was characterized by electrical and optical measurements. Whatever the excitation frequency, the discharge power was calculated from the measurements of voltage (V) and current (I) over one cycle (T) according to :

$$P = \frac{1}{T}\int_0^T V.Idt \qquad \text{Equation 2}$$

Power being calculated from the integration over one cycle of the product of the measured current and voltage, the capacitive component is equal to 0. Discharge current was measured with a current probe (Lilco LTD 13W5000 400Hz-100MHz), and voltage applied to the electrodes measured with a high voltage probe (Tektronic P6015A 75MHz) connected to a digital oscilloscope Tektronix DPO4104 (1GHz).

For low frequency excitation, results were also processed with a homemade labview program to extract the discharge current and the gas voltage [11]. For frequencies higher than 100 kHz, power delivered by the amplifier, ($P_{amp} = P_{in}-P_{ref}$ with P_{in} incident power and P_{ref} reflected power, Figure 2) could be measured with a Werlatone 50 dB Dual Directional Coupler, model C7325. This coupler was only used to adjust the frequency to minimize the reflected power and not to measure the discharge power as the measurements includes the discharge power and the transformer and circuit losses.

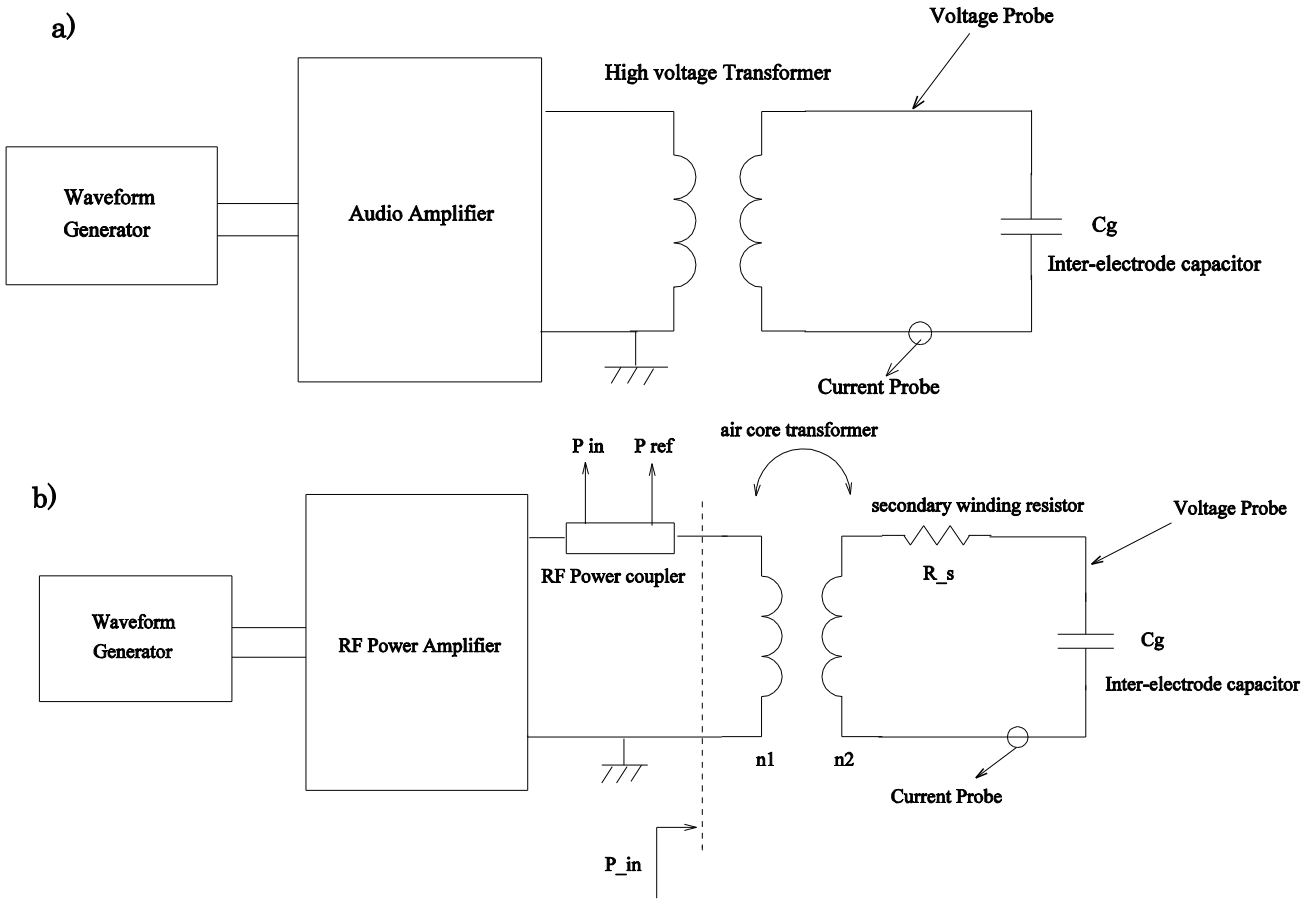

Figure 2. Electrical circuit for a) low frequency DBD and b) radiofrequency DBD (P_{in} is the incident power and P_{ref} the reflected power)

Plasma photographs were taken with an intensified CCD camera (PI-MAX II, Princeton Instruments) with a

camera lens working from 200 to 1100 nm. Exposure time could be as short as 5 ns.

3. Results

The objective of this work was to identify the different discharge regimes observed when the excitation frequency varies from 50 kHz to 9 MHz, and to correlate them with the discharge power. For a given electrode configuration and gas mixture, significant variations of breakdown voltage and power are a good indication of variation in ionization mechanisms. Fast imaging of the gas gap showing where the energy is injected also illustrate variation in discharge regime. Thus electrical measurements and fast imaging will be successively presented and analyzed.

3.1 Electrical characterization

Current and voltage oscillograms are powerful means to characterize DBDs. However, when the excitation frequency increases, the capacitive component of the current due to the solid dielectric and the gas gap becomes too high to allow the separation between this displacement current and the discharge current. This effect is illustrated in Figure 3, which presents oscillograms of the measured current, the applied voltage and the discharge light intensity. Light intensity gives a good indication of when the discharge is turned on and thus on the discharge current shape. For 50 kHz excitation, the discharge and capacitive current clearly appear on the measured current. For 550 kHz excitation, it is no longer possible to separate them. This is especially true because according to light intensity measurements, the discharge current should be sinusoidal. Thus current and voltage measurements are not so useful when the excitation frequency increases, except for the reactive power calculation.

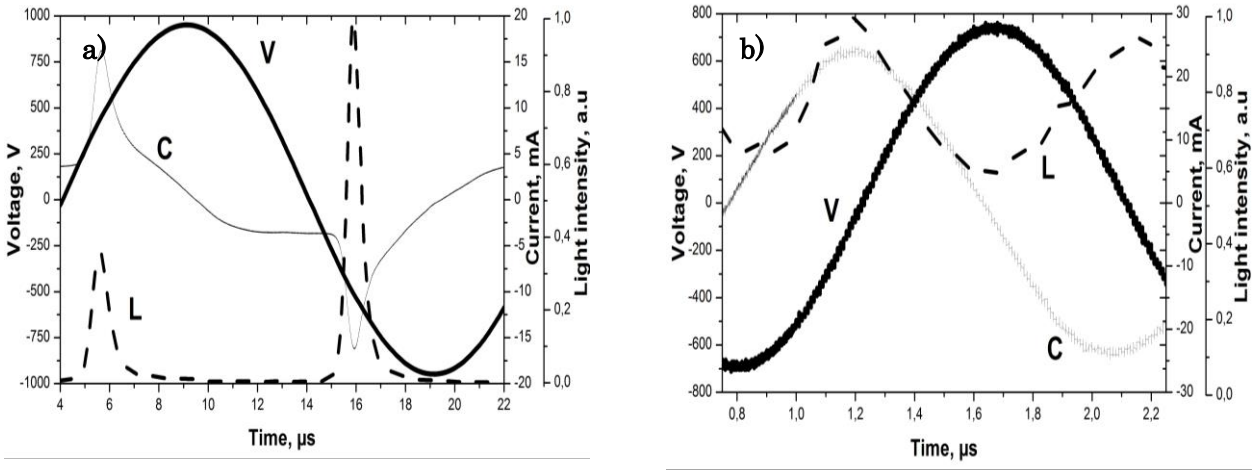

Figure 3. Comparison of the variation over one cycle of the discharge light intensity, L,(dash line) and the current, C, (thin line) and the voltage applied to the electrodes, V, (thick line) for an excitation frequency of a) 50 kHz, b) 550 kHz

Power measurement is of particular interest for a diffuse DBD because its maximum value is always limited by the transition to filamentary DBD. Microdischarge occurrence is related to current or voltage increase. For low frequency discharges it is due to a too-high ionization rate allowing the formation of large localized electronic avalanches and streamers [12]. For radiofrequency excitation it is related to the sheath gas breakdown allowing a large cathode bombardment and secondary electron emission [8]. Hence whatever the frequency, the maximum power and the voltage range over which the discharge is diffuse provides information on the discharge regime.

Discharge power was measured as a function of the voltage over the whole diffuse DBD domain for 10 different excitation frequencies ranging from 50 kHz to 7.5 MHz. Results are presented in Figure 4. Whatever the excitation frequency, the power increases with the applied voltage. To simplify the analysis in Figure 4, the slope of the curves is shown for each frequency in Figure 5. The maximum value of the power is also shown in this figure. Up to 520 kHz, the voltage and thus the power increase is limited by the transition to filamentary discharge. For higher frequencies, the maximum power is limited by the power supply.

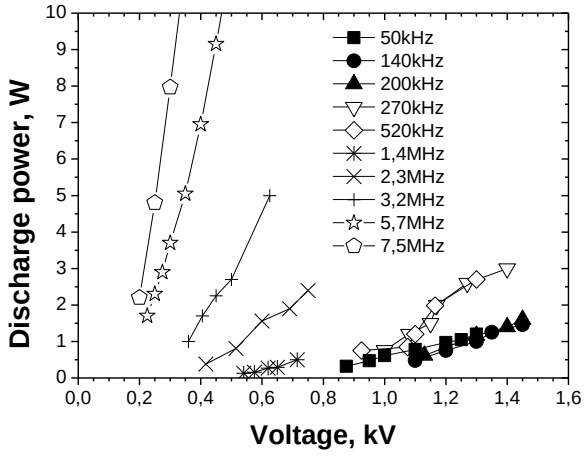

Figure 4. Discharge power as a function of the voltage applied to the electrodes for different excitation frequencies

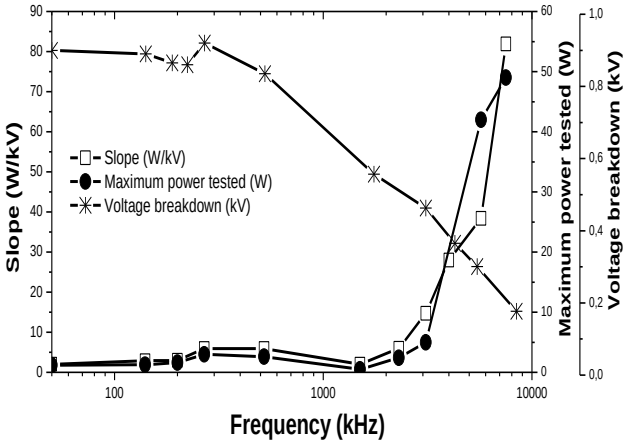

Figure 5. Power increase per kV of the applied voltage increase (slope of Figure 4), power maximum as a function of the excitation frequency and voltage breakdown

The curves of Figure 4 can be separated into 3 sets. For 50, 140 and 200 kHz, curves of the power as a function of the voltage overlap to some extent with a slope of about 2.5W/kV and a maximum power value of 1.6 W. This is for a 1.5 cm^3 plasma, and the power density reaches 1.1 W/cm^3. The breakdown voltage is almost constant at around 850 V because the polarity reverse occurs more slowly than breakdown process (10^{-6} to 10^{-8} s). The breakdown takes place as if DC discharge where the electric field is constant. It is controlled by positive ion flux on the cathode, because ions can reach the cathode during a half cycle when

secondary electrode emission is occurring. The low power difference at a given voltage shows that at least for excitation frequencies higher than 50 kHz, increasing the number of discharges per second is not a solution for increasing the power.

The 270 and 520 kHz curves form a second set of curves that have similar behavior. The slope and the maximum power are twice those observed between 50 and 200 kHz. The drastic increase in the power between 200 and 270 kHz is a clear indication of discharge regime transition. Breakdown voltage also decreases between 200 and 270kHz.

Another transition occurs between 520 kHz and 1.3 MHz. It is associated with a marked decrease in the voltage. In Figure 4, the range of the discharge voltage is shifted to lower values by a factor of 2: 900–1450 V to 350–750 V. The higher the frequency, the lower is the breakdown voltage (180 V at 8.4 MHz) and the higher is the power. Around a few megahertz, the amplitude of electron motion becomes smaller than the gap value limiting electron losses on electrodes by drift [30]. Consequently, the breakdown mechanism begins to be controlled by electron losses. The volume of the discharge being the same for 50 kHz and 7.5 MHz excitation, the power density increases by a factor of 30. For 7.5 MHz, a power of 49 W i.e. 36 W/cm^3 was measured. This is not the maximum value, as the voltage amplitude was limited by the power supply.

To summarize, for a 1 mm gap, dielectrics on each electrode and in argon with 133 ppm of NH_3, three discharge regimes are observed. The first one is observed for frequency equal to or lower than 200 kHz, the second one between 270 kHz and 520 kHz, and the third one for frequencies equal to or higher than 1.3 MHz. To identify these discharge regimes, short exposure time pictures of the gas gap will be presented and discussed.

3.2 Profile of the light intensity between the anode and the cathode

The diffuse DBD regime is usually determined by the maximum ionization rate reached by each discharge. Short exposure time pictures taken when the current or the light are maximum are a simple method to determine this ionization rate. For example, if the ionization rate is greater than 10^{10}/cm^3, a positive space charge able to localize the electrical field is created, and discharge light is localized close to the cathode, where the electrical field is maximum. If the ionization rate is lower, the electrical field can be considered uniform, and the light is maximum close to the anode [1].

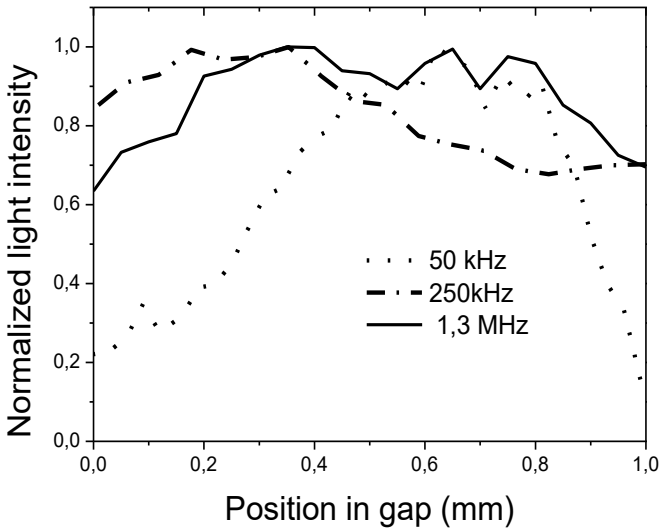

Figure 6. Light profile from the anode (on the left) to the cathode (on the right) when the light is maximum for excitation frequencies of 50 kHZ, 250 KHz and 1.3 MHz

Figure 6 presents these profiles for frequencies of 50 kHz, 250 kHz and 1.3 MHz, which correspond to the three discharge regimes determined from Figure 4. The three light profiles are different: when the frequency increases, the light maximum moves from the cathode to the anode, and then to the middle of the gap. We note that the light intensity also changes, and each profile has been normalized to its maximum to simplify the comparison.

4. Discussion

4.1. Low frequency DBDs

For the lower frequency range, the light maximum is close to the cathode, which is characteristic of a glow DBD usually observed in Penning mixtures of noble gases. The ionization rate is high enough to create a density of ions able to localize the electrical field. The formation of the cathode fall enhances ionization closer to the cathode and explains the light maximum close to it. The difference from the largely studied helium GDBD is that the positive column is not observed [1]. This is easily explained by the one-millimeter gap, too small to allow the formation of a positive column. According to the light distribution, the glow discharge observed under low frequency excitation is hindered by the small gap. It is made up of a cathode fall and a dark space with no positive column.

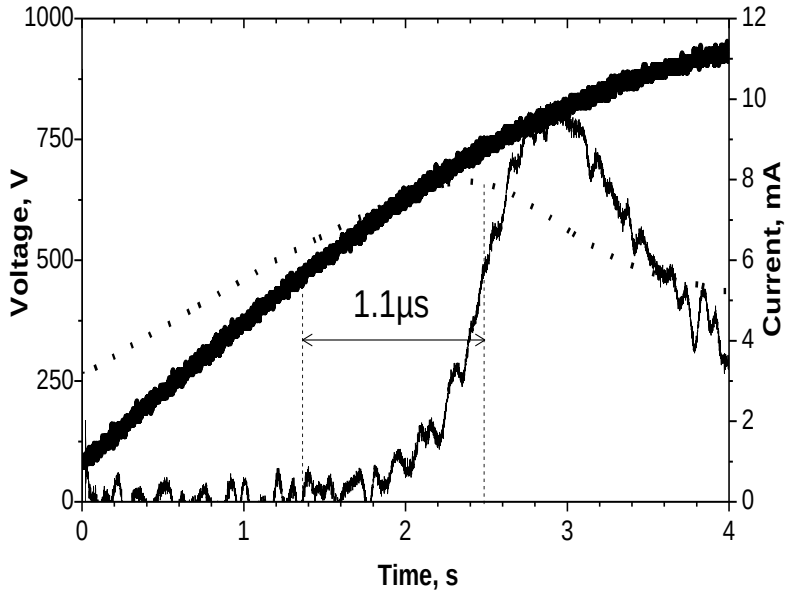

Figure 7. Details of the positive peak of the discharge current (fthin line), the gas (dot line) and applied voltage (thick line) for 50 kHz excitation showing that the time between the beginning of the discharge current increase associated with the beginning of the gas ionization and the beginning of the gas voltage decrease associated with the beginning of the cathode fall formation is 1.1 µs.

For the intermediate frequency, the light maximum always stays close to the anode. Such behavior has been previously attributed to Townsend DBDs. However, up to now TDBD has been observed only in nitrogen or air atmosphere, in which the ionization level has to be very low to avoid streamer formation; electron density is lower than 10^8 electrons /cm^3 and the excitation frequency is typically lower than 10 kHz. In such low current discharge, the density of ions is too low to distort the electric field, and so ionization is always maximum where the density of electrons is maximum, i.e. at the anode. In Penning mixtures of noble gases, higher ionization can be reached without streamer formation. However, the higher the frequency, the shorter is the time allowed for each discharge development. Thus the discharge development can be limited by the voltage oscillation frequency. The current increases during less than one quarter of the cycle, i.e. a time lapse shorter than 1 µs for 250 kHz excitation.

To try to evaluate the possible limitation of the ionization by the applied voltage oscillation, the lag between the breakdown and the formation of the cathode fall has been evaluated from discharge current and gas voltage calculated for 50 kHz. We note that this calculation cannot be done for higher frequencies (Figure 3). Gas breakdown induces current increase, and cathode fall formation induces gas voltage decrease. In Figure 7, for 50 kHz excitation, transition from Townsend to glow takes 1.1 µs, which is longer than the quarter of the cycle at 250 kHz. This time should also be compared with the time an ion takes to cross the gap. First the nature of the dominant ion has to be determined. At atmospheric pressure the rate of the reaction $Ar^+ + 2Ar \rightarrow Ar_2^+ + Ar$ is $1.5 \times 10^8\ s^{-1}$, which is very rapid compared with the microsecond timescale

of the discharge. Another reaction that has to be considered to determine the nature of the dominant ion is the charge transfer from Ar_2^+ to NH_3. For 133 ppm of NH_3 this reaction frequency is 4.23×10^6 s^{-1}, so that NH_3^+ is the dominant ion. Figure 8 compares half cycle and the time an ion takes to cross the gap. The calculation is done assuming a Laplacian field (V/d with V =voltage, d = gas gap). For each frequency, the voltage is taken as equal to the voltage used for plasma photographs in Figure 6. The mobility of NH_3^+ ion is taken equal to 3.2 cm^2/Vs. For 250 kHz, the typical time for an ion to move from the anode to the cathode is 2.2 µs, which is longer than the half cycle (2µs), while for 200 kHz it is shorter. Thus the ion accumulation close to the cathode decreases when the frequency increases, up to the point where their density is too low to generate the cathode fall consistent with the change in breakdown voltage behavior around this point; The discharge becomes a Townsend discharge. The field is uniform and high. There are fewer electrons, but they have a higher energy, which contributes to the power step when the discharge regime changes from glow to Townsend.

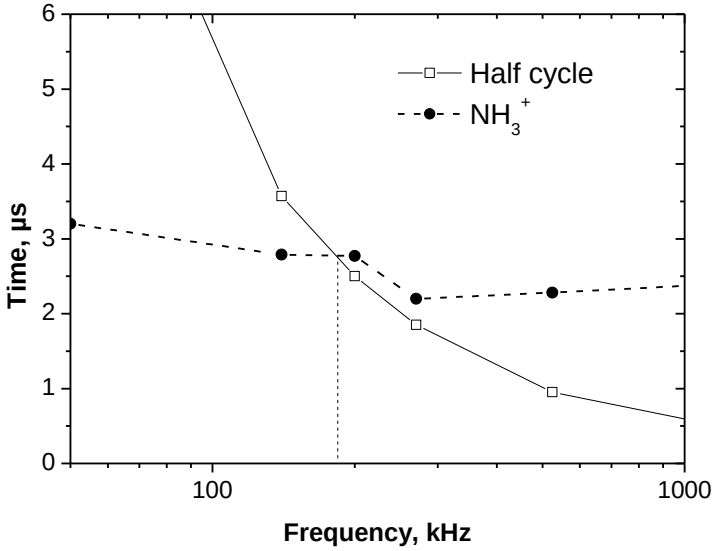

Figure 8. Comparison of the half cycle and the time an ion takes to cross the gap (dash line) as a function of the excitation frequency. Calculation is done assuming that the field is equal to the Laplatian field (V/d with V =voltage, d = gas gap) and the voltage is taken as equal to voltage used for plasma photographs (Figure 6).

In N_2 TDBDs the power is typically 10 times greater than in He GDBDs. This difference has been partly attributed to the reduction of the ratio of the DBD "time on" to "time off". To evaluate the evolution of this ratio, light intensity was measured over one cycle for the different excitation frequencies. Results for 50 kHz and 550 kHz are presented in Figure 3, showing that the time between two discharges was markedly lower for 550 kHz. From these measurements the "time on" was taken equal to the width at half height of the light peak. Figure 9 presents the ratio of this time to the width at half height of the voltage. According to this graph the influence of the discharge transition is negligible compared with the excitation frequency. From the comparison of Figure 8 and Figure 9, looking at the results associated with the GDBD, it can also

be deduced that the large decrease in the DBD “time off” slightly increases the power.

Obtaining a TDBD in Ar is a surprising result, as up to now TDBDs have only been observed in N_2 or air. N_2 TDBD is only obtained under low excitation frequencies, and Ar-NH_3 TDBD is only obtained under high excitation frequencies, but in both cases, the discharge development is limited by the power supply. In nitrogen it is the current that is limited [13], in Ar-NH_3 it is the discharge duration. In both cases the power supply limits the maximum ionization rate. Ion trapping due to frequency increase avoids cathode fall formation and limits cathode secondary emission.

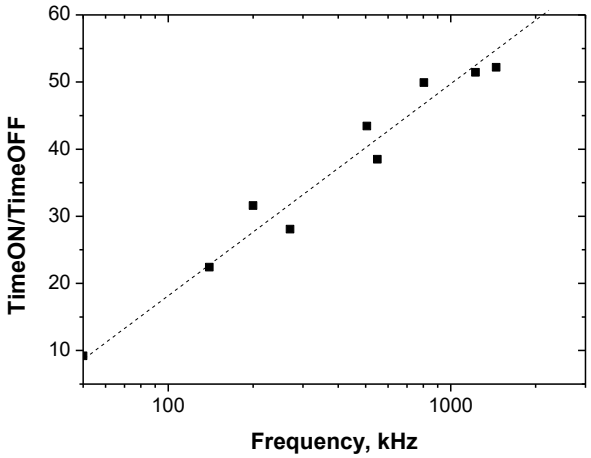

Figure 9. Ratio of width at half height of the discharge light peak and half cycle as a function of the excitation frequency

4.2 Radiofrequency DBD

When the frequency reaches 1.3 MHz, the breakdown voltage decreases, showing that a new ionization mechanism significantly contributes. In Figure 6, ionization is maximum in the gas bulk. This is in agreement with a radiofrequency behavior. According to the literature, different ionization mechanisms can be involved in an atmospheric pressure non-equilibrium radiofrequency discharge: (i) during sheath expansion electrons are accelerated towards the opposing electrode, and cause excitation/ionization adjacent to the expanding sheath edge [14], (ii) at the time of maximum sheath voltage, excitation and ionization by secondary electrons can occur at both sheaths [15,16,17], (iii) excitation can also be observed at each electrode during sheath collapse [18], attributed at low pressure in molecular gases to the electric field reversal localized at the sheath edge and caused by electron-neutral collisions [19] (at atmospheric pressure the field is not reversed because of lower species diffusion),and (iv) significant excitation and ionization inside the bulk at the times of fastest sheath expansion are also observed [20, 18], correlated to a rather high bulk field due to

a highly collisional medium; this behavior is similar to that observed for a low pressure RF discharge in electronegative gases [21].

Dominant mechanisms depend on the amplitude of the voltage or on the power. In such condition, the excitation during sheath expansion is assumed to be stronger than the gamma emission from the cathode. This assumption is supported by two observations: (i) the low emission close to the electrodes, and (ii) the similarity of the discharge behavior whatever the nature of the cathode: for 50 kHz excitation, filamentary discharge are observed if a silicon wafer is added on the dielectric surface in contact with the plasma [22]. For RF excitation the adding of a silicon wafer has no influence. The bulk excitation observed in Figure 6 presumes ionization adjacent to the expanding sheath edge due to wave riding and ionization in the bulk, resulting from a high bulk electric field attributed to the low conductivity related to a high electron-neutral collision frequency in the gas bulk at atmospheric pressure [21]. At low power, electron heating in the bulk is the main mechanism.

To confirm this interpretation, it is of interest to compare the gas gap and the amplitude of electron motion determined from transport Equation 3, which is the sum of diffusion and drift motion:

$$n_e v_e = -D_e \nabla \mathbf{n_e} - \mathbf{n_e} \mu_e \mathbf{E} \qquad \text{Equation 3}$$

D_e is the electron diffusion coefficient, μ_e the electron mobility, and E the electric field. Equation 3 can be approximated by removing the diffusion term to calculate the electron displacement due to the electric field, as done by other authors [23, 24]:

$$v_e = -1.414 \mu_e \frac{V}{d} \cos(wt) \qquad \text{Equation 4}$$

$$A \approx 1.414 \langle \mu_e \rangle \frac{V}{wd} \qquad \text{Equation 5}$$

With, A, the amplitude of electron oscillation, V, voltage amplitude and, w, angular frequency. Electron mobility is 340 $cm^2/(V.s)$ [25].

Figure 10 presents the calculation results for V equal to the minimum breakdown voltage according to Figure 5. The amplitude of electron motion during half cycle decreases from 27 mm at 50 kHz to 160 µm at 8.4 MHz. It is equal to the gas gap for about 3.5 MHz. In Figure 10, the time for electrons to cross the gas gap is equal to the half cycle duration for 5 MHz. This time is equal to 100 ns, which is 30 times longer than that of ions while the mobilities ratio is 100. The difference is due to the decrease of the breakdown voltage with frequency increase.

For frequencies between 3 and 5 MHz, electron oscillation by drift becomes similar to the gap value, and

the higher the excitation frequency, the more marked is their confinement in the gas bulk [26, 27]. The disappearance of electron loss due to electron drift to the anode explains the electron density increase, and the power increase when the bulk ionization increases. The main ionization mechanism occurs in the plasma bulk without direct contribution of the electrodes, whereas for lower excitation frequency, cathode secondary emission and electron drift to the anode play a dominant role.

Experimental results show that at 1.3 MHz, both the discharge power (Figure 4) and the discharge light emission are low. However, the light is emitted by the gas bulk (6) in agreement with RFDBD behavior. According to the calculation, at that frequency, the amplitude of electron motion during the half cycle is 2 mm, so for a 1 mm gap the low discharge power can be explained by a rather large loss of electrons at the anode, caused by drift. The contribution of cathode secondary emission is low, but there are still electron losses at the anode. This loss decreases when the frequency increases, explaining both the breakdown voltage reduction and the power and light intensity increase.

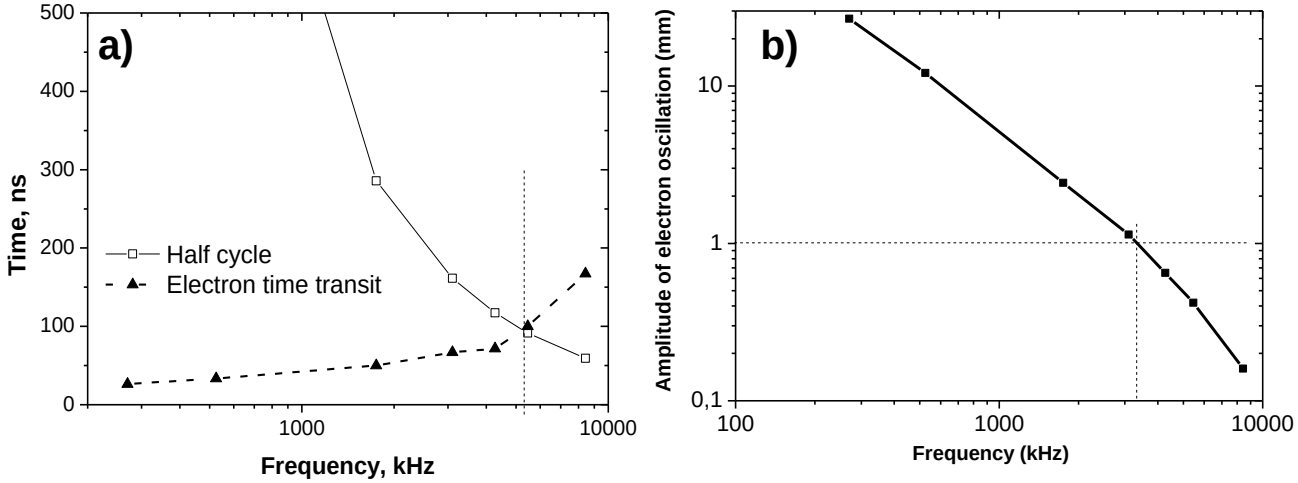

Figure 10. a) Comparison of the half cycle and the time an electron takes to cross the gap, and b) calculated amplitude of electron motion as a function of the excitation frequency. The horizontal line indicates 1 mm, which is the gas gap. Calculation assumes a Laplacian field (V/d with V =voltage, d = gas gap), and the voltage is taken as equal to the maximum voltage giving the diffuse DBD.

A rather surprising conclusion of this work was drawn from a significant difference between the low frequency regime and the glow regime: in the frequency range studied, namely the high part of GDBD and the low part of RFDBD, the excitation frequency had a limited influence on the power of the former, but a large influence on the latter. This observation is quite surprising, because in the low frequency regime the discharge is pulsed, and an increase in the power with the discharge rate was expected, whereas in the RF mode the discharge is always on.

In conclusion, observation of the power evolution with the applied voltage and the light distribution in the

gas gap for different excitation frequency reveals three different diffuse DBD regimes in Ar-NH_3 Penning mixture discharge occurring in a 1 mm gap: a hindered glow DBD occurring for frequency excitation typically lower than 200 kHz, a Townsend DBD typically observed between 250 kHz and 500 kHz, and a radio frequency DBD for frequencies higher than 1.3 MHz. The transition from glow to Townsend is attributed to the reduction of the time allowed to discharge development; the transition from Townsend to RF is attributed to the acceleration of electrons in plasma bulk because of high field due to highly collisional conditions, and by the rapid sheath motion at higher power.

5. Conclusion

The influence of the excitation frequency on the behavior of a homogeneous DBD in Ar/$NH_3$was studied from low frequency (50 kHz) to radiofrequency (9 MHz). Photographs show that a homogeneous discharge free of microdischarge was obtained whatever the frequency.

Three different discharge regimes were identified from electrical and optical measurements. When the frequency increased, the discharge transited from GDBD to TDBD and then RFDBD. The transition from GDBD to TDBD was abrupt and related to ion trapping in the gas gap. Thus in a noble gas Penning mixture, increasing the excitation frequency is a way to limit the ionization level while increasing the power. This is true until electrons begin to be trapped and ionization begins to be controlled by sheath oscillations. This transition from TDBD to RFDBD is associated with a drastic increase in the power, related to higher electron density.

For a 1 mm gap in Ar + 133 ppm NH_3 mixture, glow to Townsend transition occurred between 200 and 250 kHz ,and RFDBD was observed from 1.3 MHz. For low frequency DBDs, in the 50 kHz to 520 kHz range, the power, which depends slightly on the frequency, varied markedly with the discharge regime: a factor of 2 was observed between GDBD and TDBD. RFDBD power was lower than that for low frequency DBD when electron trapping was limited, but it reached 35 W/cm^3 for the highest frequency tested. This high value was certainly not the maximum. This large power increase was associated with a decrease in the breakdown voltage by a factor of 3, reflecting the variation of the dominant ionization mechanisms and electric field distribution over the gas gap. Electron density decreases between GDBD and TDBD, while electron energy increases because of the field uniformity. On the contrary, in the RFDBD the electron density is expected to be markedly higher, and with a lower electron energy. Work is in progress to confirm these points.

6. Acknowledgement

The authors thank the Agence Nationale de la Recherche (ANR) for its support of the PREPA project (Grant No ANR-09-BLAN-0043-03).

7. References

[1] F. Massines, N. Gherardi, N. Naudé, P. Ségur, Eur. Phys. J. Appl. Phys. 47(2), 22805, (2009)

[2] N. Gherardi and F. Massines, IEEE Trans. Plasma Sci., 29, 536 (2001)

[3] S. Okazaki, M. Kogoma, M. Uehara and Y. Kimura, J. Phys. D: Appl. Phys. 26, 889 (1993)

[4] J. J Shi and M. G. Kong, Applied physics letters 90, 111502 (2007), Radiofrequency dielectric barrier glow discharges in atmospheric argon

[5] J. J. Shi, D.W. Liu, and M.G. Kong, Applied physics letters 90, 031505 (2007), Mitigating plasma constriction using dielectric barriers in radiofrequency atmospheric pressure glow discharges

[6] B. Li, Q. Chen and Z. W. Liu, Applied physics letters 96, 041502 (2010); doi:10.1063/1.3299010, A large gap of radio frequency dielectric barrier atmospheric pressure glow discharge

[7]Berchtikou, A. Lavoie, J. Poenariu, V. Saoudi, B. Kashyap, R. Wertheimer, M.R., Dielectrics and electrical insulator, IEEE, 18, ISSN 1070-9878 (2011), Thermometry in noble gas dielectric barrier discharges at atmospheric pressure using optical emission spectroscopy

[8] J. J. Shi and M.G. Kong, Applied physics letters 90, 101502 (2007), Mode transition in radiofrequency atmospheric argon discharges with and without dielectric barriers

[9] M. Morajev, R. F. Hicks, Chem. Vap.Deposition 2005,11, 469...476

[10] H Caquineau, I. Enache, N. Gherardi, N. Naudé and F. Massines, J. Phys. D: Appl. Phys. 42 125201 (2009)

[11] N. Naudé, J.P. Cambronne, N. Gherardib, and F. Massines, Eur. Phys. J. Appl. Phys. 29, 173–180 (2005)

[12] A. Chirokov, A. Gutsol, and A. Fridman, Pure Appl. Chem., Vol. 77, No. 2, pp. 487–495, 2005.
DOI: 10.1351/pac200577020487, Atmospheric pressure plasma of dielectric barrier discharges

[13] F. Massines, Et. Es-sebbar, N. Gherardi, N. Naudé, D. Tsyganov, P. Ségur, S. Pancheshnyi, 35th EPS Conference on Plasma Phys. Hersonissos, 9 - 13 June 2008 ECA Vol.32D, P-2.169 (2008)

[14] Iza F., Lee J. K. and Kong M. G. 2007, Phys. Rev Lett. 99 031501

[15] Waskoeing J, Niemi K, Knake N., Graham L M, Reuter, Schultz-von der Gathen V and Gans T., 2010, plasma Source Sci. Technol. 19 045018

[16] Nierman B, Hemke T, Babaeva N Y, Böke M, Kushner M J Mussembrock T and Winter J, 2011, J. Phys D: applied physic. 44 485204

[17] Niemi K, Waskoenig J, Sadegui N, Gans T, and D O'Connell 2011 Plasma Sources Sci. Technol. 20 055005

[18] Liu D W, Iza F and Kong M G 2008 Applied Physics Letters 93 261503

[19] Schulze J, Derzsi A, Dittmann K, Hemke T, Meichsner J and Donko Z 2011 Phys Rev Lett. 107 275001

[20] Benedikt J, Hofmann S, Knake N, Böttner H, Reuter R, von Keudell A, Schultz-von der Gathen V 2010 Eur. Phys. J D 60 539

[21] T. Hemke, D. Eremin, T Mussenbrock, A Derzi, Z Donko, K Dittman, J Meichsner, J Schulze, arXiv:1208.6519v1 [physics.plasm-ph] 31 Aug 2012

[22] N. Naudé and F. Massines, IEEE transaction on Plasma Science, Vol36, N°4, August2008, 1322-1324

[23] J. Park, I. Henins, H. W. Herrmann, and G. S. Selwyn, J. Appl. Phys., DOI: 10.1063/1.1323754#

[24] J. Zhang, K. Ding and K. Wei. J. Zhang and J. Shi, Phys. of plasmas 16, 090702 (209); doi:10.1063/1.3240350, Excitation frequency dependent mode manipulation in radiofrequency atmospheric argon glow discharge.

[25] P Kloc, H.E Wagner, D Trunec, Z Navratil and G Fedoseev, Journal of Physics D: Applied Physics 43, 34 (2010) 345205

[26] J. L. Walsh, Y. T. Zhang, F. Iza, and M. G. Kong, Applied physics letters 93, 221505-2008, Atmospheric-pressure gas breakdown from 2 to 100 MHz

[27] D. W. Liu, J. J. Shi, and M. G. Kong, Appl. Phys. Lett.90, 041502 (2007), Electron trapping in radiofrequency atmospheric-pressure glow discharges

[28] Hiroaki Kakiuchi, Hiromasa Ohmi and Kiyoshi Yasutake, J. Vac. Sci. Technol. A 32, 030801 (2014), Atmospheric-pressure low-temperature plasma processes for thin film deposition

[29] S A Starostin, P Antony Premkumar, M Creatore, E M van Veldhuizen, H de Vries, R M J Paffen and M C M van de Sanden, Plasma Sources Sci. Technol. (2009) 18 045021. doi:10.1088/0963-0252/18/4/045021, On the formation mechanisms of the diffuse atmospheric pressure dielectric barrier discharge in CVD processes of thin silica-like films

[30] Nasser, E., 1971. Fundamentals of gaseous ionization and plasma electronics, ed. (John Wiley and Sons, Inc).